

Formation of Fe(III)Fe(IV) Species from the Reaction between a Diiron(II) Complex and Dioxygen: Relevance to Ribonucleotide Reductase Intermediate X

Dongwhan Lee,[†] J. Du Bois,[†] Doros Petasis,[‡] Michael P. Hendrich,[‡] Carsten Krebs,[§] Boi Hanh Huynh,[§] and Stephen J. Lippard^{*†}

Department of Chemistry
Massachusetts Institute of Technology
Cambridge, Massachusetts 02139

Department of Chemistry, Carnegie Mellon University
Pittsburgh, Pennsylvania 15213

Department of Physics, Emory University
Atlanta, Georgia 30322

Received July 8, 1999

The reaction of *m*-terphenyl-based carboxylic acids with ferrous salts produces novel tetracarboxylate dinuclear clusters through an extraordinarily efficient self-assembly process. Recently, we reported the preparation of one such compound, [Fe₂(μ-O₂-CAr^{Tol})₂(O₂CAr^{Tol})₂(C₅H₅N)₂] (1), and highlighted its unique reactivity with dioxygen.¹ Efforts to explore this chemistry further were hampered by the poor solubility of 1 in nonpolar solvents, thus prompting the synthesis of new Ar^{Tol}CO₂⁻-derived adducts. Here we describe a tetracarboxylate-bridged complex, [Fe₂(μ-O₂-CAr^{Tol})₄(4-^tBuC₅H₄N)₂] (2), that reacts with O₂ to furnish [Fe₂(μ-OH)₂(μ-O₂CAr^{Tol})₂(O₂CAr^{Tol})₂(4-^tBuC₅H₄N)₂] (4). This process parallels the oxygenation reaction of 1, proceeding through a metastable green intermediate 3 that decays to afford 4 in isolated yields exceeding 75%. Studies with 2 have made possible the characterization and assignment of 3 as a mixture containing equimolar quantities of mixed-valent species Fe^{III}Fe^{IV} and Fe^{II}-Fe^{III}. The formation of a high-valent diiron cluster from 2 and dioxygen mimics closely the purported mechanistic chemistry of certain diiron metalloenzymes.² Additionally, the Fe^{III}Fe^{IV} component in 3 represents a putative model for a key intermediate, X, in the reaction cycle of the R2 subunit of ribonucleotide reductase (RNR-R2).^{3,4} To the best of our knowledge, the formation of 3 is the first example of a process that utilizes dioxygen to access the Fe^{IV} oxidation state in synthetic model complexes.⁵

Neutral tetracarboxylate complex 2 was prepared upon treatment of [Fe₂(μ-O₂CAr^{Tol})₂(O₂CAr^{Tol})₂(THF)₂]¹ with 2 equiv of 4-*tert*-butylpyridine (Scheme 1). The structure of 2 reveals a dinuclear adduct in which four Ar^{Tol}CO₂⁻ groups span the two metal centers (Figure S1). Each iron in 2 is square pyramidal and has a coordination geometry that closely resembles those of previously reported diiron(II) paddlewheel complexes.⁶

[†] Massachusetts Institute of Technology.

[‡] Carnegie Mellon University.

[§] Emory University.

(1) Lee, D.; Lippard, S. J. *J. Am. Chem. Soc.* **1998**, *120*, 12153–12154.

(2) (a) Feig, A. L.; Lippard, S. J. *Chem. Rev.* **1994**, *94*, 759–805. (b) Wallar, B. J.; Lipscomb, J. D. *Chem. Rev.* **1996**, *96*, 2625–2657. (c) Valentine, A. M.; Lippard, S. J. *J. Chem. Soc., Dalton Trans.* **1997**, 3925–3931. (d) Que, L., Jr. *J. Chem. Soc., Dalton Trans.* **1997**, 3933–3940.

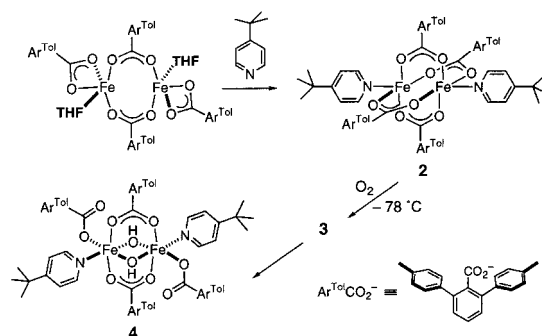
(3) Riggs-Gelasco, P. J.; Shu, L.; Chen, S.; Burdi, D.; Huynh, B. H.; Que, L., Jr.; Stubbe, J. *J. Am. Chem. Soc.* **1998**, *120*, 849–860.

(4) Stubbe, J.; van der Donk, W. A. *Chem. Rev.* **1998**, *98*, 705–762.

(5) Bis(μ-oxo)diiron(III, IV) complexes were prepared by oxidizing diiron(III) complexes with H₂O₂ at low temperature: (a) Dong, Y.; Fujii, H.; Hendrich, M. P.; Leising, R. A.; Pan, G.; Randall, C. R.; Wilkinson, E. C.; Zang, Y.; Que, L., Jr.; Fox, B. G.; Kauffmann, K.; Münck, E. *J. Am. Chem. Soc.* **1995**, *117*, 2778–2792. (b) Dong, Y.; Que, L., Jr.; Kauffmann, K.; Münck, E. *J. Am. Chem. Soc.* **1995**, *117*, 11377–11378. (c) Hsu, H.-F.; Dong, Y.; Shu, L.; Young, V. G., Jr.; Que, L., Jr. *J. Am. Chem. Soc.* **1999**, *121*, 5230–5237.

(6) Randall, C. R.; Shu, L.; Chiou, Y.-M.; Hagen, K. S.; Ito, M.; Kitajima, N.; Lachicotte, R. J.; Zang, Y.; Que, L., Jr. *Inorg. Chem.* **1995**, *34*, 1036–1039.

Scheme 1



Oxygenation of a CH₂Cl₂ solution of 2 at –78 °C resulted in the irreversible generation of a deep green solution 3 with a broad visible absorption centered at ~670 nm ($\epsilon = 1700 \text{ M}^{-1} \text{ cm}^{-1}$). At low temperature, 3 is stable for >12 h, but it slowly decays upon warming above –65 °C to afford a yellow material (Figure S2). X-ray analysis established this product to be the bis(μ-hydroxo)diiron(III) complex 4 (Scheme 1 and Figures S3, S4). Compound 4 is structurally analogous to that obtained from oxidation of 1,¹ having a short Fe^{III}–Fe^{IV} separation of ~2.84 Å due to the presence of four bridging ligands. A weak ferromagnetic interaction, $J = 0.63(5) \text{ cm}^{-1}$ with $g = 2.00(1)$,⁷ was observed by SQUID susceptometry on solid samples of 4.

X-Band EPR spectra collected on frozen CH₂Cl₂ samples of 3 exhibited a strong isotropic $g = 2$ signal and a less intense absorption at $g = 10$ (Figure 1). Quantitation of these two species accounted for 70% of the total iron, the former signal contributing 40% and the latter 30%. The X-band signal at $g = 2$, with a width of ~28 G, originates from an $S = 1/2$ species which shows resolved g -anisotropy at Q-band (see inset). The two simulations overlaid on the data use the same parameter set of $g = 1.986$, 1.997, and 2.011. This g -anisotropy is similar to that of the RNR-R2 X ($g = 1.994$, 1.999, and 2.007) signal,^{8,9} which arises from the antiferromagnetically coupled Fe^{III}Fe^{IV} core in this enzyme intermediate. The signals at $g = 10$ (X- and Q-band) and $g = 4.3$ and 2.8 (Q-band) originate from an $S = 9/2$ species, and the simulations overlaid on the data were obtained with $D = 1.2 \text{ cm}^{-1}$, $E/D = 0.013$, and $g = 2.00$.¹⁰ Both the $S = 1/2$ and $S = 9/2$ signals display Curie law behavior up to 150 K, indicating exchange interactions of $|2J| > 200 \text{ cm}^{-1}$ for the former and $> 50 \text{ cm}^{-1}$ for the latter.⁷ The similarity of the $S = 9/2$ EPR signal with that of a complex prepared by one-electron chemical oxidation of 2¹¹ leads us to assign it as the corresponding Fe^{II}Fe^{III} cation. The $S = 9/2$ spin state can result either from a ferromagnetic interaction between iron centers or by electron delocalization for which a double-exchange mechanism¹² is dominant.

Figure 2 displays the Mössbauer spectra of a solid powder sample of 3 recorded at 4.2 K with a 50-mT magnetic field applied parallel (A) and perpendicular (B) to the γ -rays. The spectra may be deconvoluted into three major components. A central quadrupole doublet (marked by brackets) with apparent Mössbauer parameters of $\Delta E_Q = 1.13 \text{ mm/s}$ and $\delta = 0.54 \text{ mm/s}$ is assigned

(7) $H = -2JS_1 \cdot S_2$.

(8) Burdi, D.; Sturgeon, B. E.; Tong, W. H.; Stubbe, J.; Hoffman, B. M. *J. Am. Chem. Soc.* **1996**, *118*, 281–282.

(9) Sturgeon, B. E.; Burdi, D.; Chen, S.; Huynh, B. H.; Edmondson, D. E.; Stubbe, J.; Hoffman, B. M. *J. Am. Chem. Soc.* **1996**, *118*, 7551–7557.

(10) The resonances near $g = 4$ in Q-band for both parallel and perpendicular modes are from an intradoublet transition and are not included in the simulation. The $g = 19$ (X-band) and possibly the $g = 29$ (Q-band) signals are from the diiron(III) species, whereas the $g = 16$ signal (Q-band) and its simulation are from unreacted 2, which account for 20 and 10% of the total iron, respectively.

(11) Lee, D.; Lippard, S. J., manuscript in preparation.

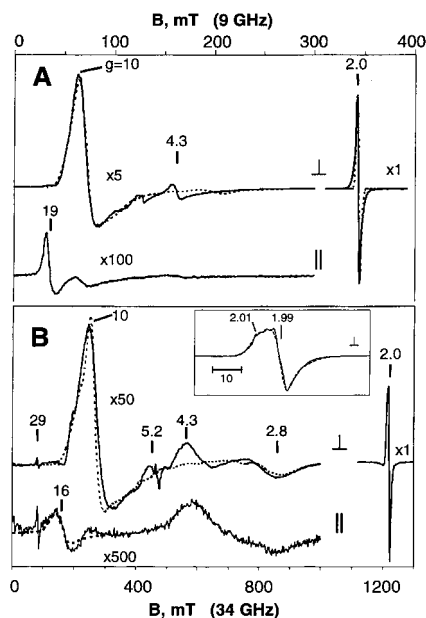


Figure 1. X-band (A, 9.4 GHz) and Q-band (B, 34.1 GHz) EPR spectra of a frozen CH_2Cl_2 solution of **3** for microwave fields parallel and perpendicular to the static field. Dashed lines are quantitative simulations for the $S = 1/2$ and $S = 3/2$ species discussed in the text. The inset is a magnified view of the Q-band $g = 2$ signal. Sample temperatures are < 12 K and relative signal gains are shown on the figure.

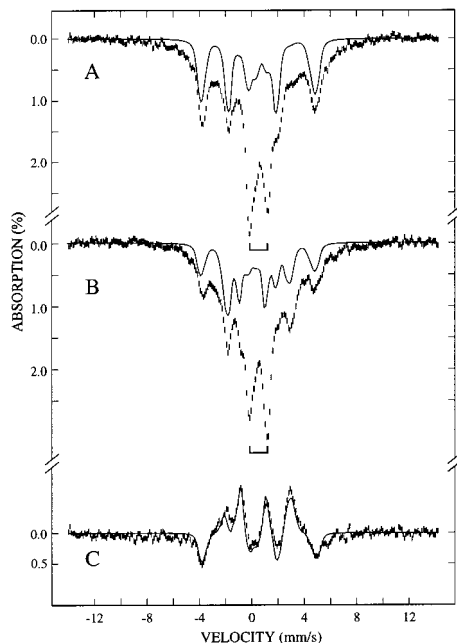


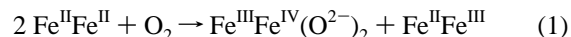
Figure 2. Mössbauer spectra of the solid powder sample of **3** recorded at 4.2 K with a 50-mT magnetic field applied parallel (A) and perpendicular (B) to the γ -rays. Spectrum C is a difference spectrum of the spectra shown in A and B. The solid lines are theoretical simulations of the $S = 1/2$ species using the parameters listed in Table S1. The theoretical spectra are normalized to 36% of the total iron absorption.

to an antiferromagnetically coupled diferric species (30% of total iron). A magnetically split spectrum with well-resolved peaks at -3.8 , -1.7 , $+2.0$, and $+4.9$ mm/s can be assigned to the $S = 1/2$ species (36% of total iron). The remaining component (34% of total iron) is a broad and featureless spectrum with absorption extending from -7 mm/s to $+7$ mm/s.¹³ Of the three diiron

(12) Münck, E.; Papaefthymiou, V.; Surerus, K. K.; Girerd, J.-J. *Metal Clusters in Proteins*; Que, L., Jr., Ed.; American Chemical Society: Washington, D. C., 1988; pp 302–325.

species mentioned above, only the spectrum of the $S = 1/2$ species is expected to have a strong dependence on the orientation of the applied field with respect to the direction of the γ rays. Consequently, a difference spectrum (C of Figure 2) of the spectra A and B of Figure 2 will cancel most of the contributions from the other species and reveal the field orientation dependence of the $S = 1/2$ species. Analysis of the data yields parameters that compare very well with previously reported RNR-R2 X, MMOH-Q_X, and a related $\text{Fe}^{\text{III}}\text{Fe}^{\text{IV}}$ model compound (Table S1).^{5b,9,14} In particular, the observed isomer shifts, 0.55 and 0.12 mm/s, for the two iron sites indicate unambiguously that the $S = 1/2$ component is an $\text{Fe}^{\text{III}}\text{Fe}^{\text{IV}}$ species.

A mechanism that accounts for the formation of equal amounts of $\text{Fe}^{\text{III}}\text{Fe}^{\text{IV}}$ and $\text{Fe}^{\text{II}}\text{Fe}^{\text{III}}$ species in **3** assumes that a portion of **2** reduces some oxidized iron before all of this starting diiron(II) complex can react with dioxygen. The balanced reaction (eq 1) indicates that only $1/2$ equiv of O_2 is needed to generate $1/2$ mol $\text{Fe}^{\text{III}}\text{Fe}^{\text{IV}}$ and $1/2$ mol $\text{Fe}^{\text{II}}\text{Fe}^{\text{III}}$ from 1 mol of **2**.¹⁵ Under the reaction



conditions, a certain percentage of an $\{\text{Fe}_2\text{O}_2\}^{4+}$ adduct (or some equivalent) would form in the presence of unreacted **2**. Single electron-transfer from **2** to this adduct would result in two different mixed-valent species, $\text{Fe}^{\text{III}}\text{Fe}^{\text{IV}}$ and $\text{Fe}^{\text{II}}\text{Fe}^{\text{III}}$.¹⁶ Although the proposed reaction model for **2** is speculative, both the EPR and Mössbauer data offer compelling evidence for the formation of a high-valent $\text{Fe}^{\text{III}}\text{Fe}^{\text{IV}}$ product upon low-temperature oxygenation of this complex.^{17,18}

In conclusion, we have demonstrated that the tetracarboxylate diiron(II) complex **2** is able to react directly with dioxygen to form high-valent iron species. The chemistry of this model system is unique and parallels closely the function of the diiron cofactor in the R2 subunit of RNR. These results are testament to the utility of 2,6-diarylbenzoate ligands for the assembly of diiron compounds with unprecedented reactivity.

Acknowledgment. This work was supported by grants from the National Science Foundation and National Institute of General Medical Sciences. We thank Drs. T. J. Mizoguchi and B. Spingler for helpful discussions.

Supporting Information Available: Details of the synthetic procedures, X-ray crystallographic tables, physical characterization of **2** and **4** (PDF). An X-ray crystallographic file in CIF format. This material is available free of charge via the Internet at <http://pubs.acs.org>.

JA9923686

(13) Preliminary high-field Mössbauer data indicate this broad component to be a valence-delocalized $S = 3/2$ $\text{Fe}^{\text{II}}\text{Fe}^{\text{III}}$ species, detailed characterization of which is currently in progress.

(14) Valentine, A. M.; Tavares, P.; Pereira, A. S.; Davydov, R.; Krebs, C.; Hoffman, B. M.; Edmondson, D. E.; Huynh, B. H.; Lippard, S. J. *J. Am. Chem. Soc.* **1998**, *120*, 2190–2191.

(15) In support of this putative reaction scheme, manometric measurements demonstrated that substoichiometric amounts of O_2 (0.75 ± 0.1) are consumed per mol of **2** to provide **3**. At present, however, we have no apparent explanation for the formation of the diiron(III) species. It might be generated by a reaction between the $\text{Fe}^{\text{II}}\text{Fe}^{\text{III}}$ and $\text{Fe}^{\text{III}}\text{Fe}^{\text{IV}}$ species or in a branching pathway involving **2** and dioxygen.

(16) A related model has been recently proposed for the generation of Y122• in RNR-R2, in which two functionally different diiron clusters are involved in the reaction with O_2 : Miller, M. A.; Gobena, F. T.; Kauffmann, K.; Münck, E.; Que, L., Jr.; Stankovich, M. T. *J. Am. Chem. Soc.* **1999**, *121*, 1096–1097.

(17) The oxidizing ability of **3** was manifested by reactions with substituted phenols, 2,4,6-tri-*tert*-butylphenol or 2,4-di-*tert*-butylphenol, which provided the corresponding phenoxyl radical (10%) or biphenol coupled product (40%), respectively. Unpublished results.

(18) In this regard it is interesting to note that reaction of O_2 with a similar diiron(II) complex derived from 2,6-dimesitylbenzoic acid affords an EPR silent purple complex. This species has been assigned as a diiron(III) peroxide on the basis of an isotope-sensitive vibration at 885 cm^{-1} in the resonance Raman spectrum: Hagadorn, J. R.; Que, L., Jr.; Tolman, W. B. *J. Am. Chem. Soc.* **1998**, *120*, 13531–13532.